

Fifth Quarterly Report  
for

## SOLAR CELL COVER GLASS DEVELOPMENT

(1 October 1967 through 1 April 1968)

Contract Number: NAS5-10236

Prepared by:

Ion Physics Corporation  
Burlington, Massachusetts

Prepared for:

Goddard Space Flight Center  
Greenbelt, Maryland

N71-73703

(ACCESSION NUMBER)

(THRU)

32  
(PAGES)

None  
(CODE)

CR-118413  
(NASA CR OR TMX OR AD NUMBER)

(CATEGORY)

FACILITY FORM 602



**ION** PHYSICS CORPORATION



A Subsidiary of High Voltage Engineering Corporation

BURLINGTON, MASSACHUSETTS

Quarterly Technical Progress Report No. 5

1 October 1967 through 1 April 1968

SOLAR CELL COVER GLASS DEVELOPMENT

National Aeronautics and Space Administration  
Goddard Space Flight Center  
Greenbelt, Maryland

Contract NAS5-10236

Project Manager: Roger W. Sudbury  
R. Sudbury

ION PHYSICS CORPORATION  
BURLINGTON, MASSACHUSETTS

## OBJECTIVE

The objective of this program is refinement and economic optimization of techniques for fabrication of thick integral coverslips for silicon solar cells. An a priori assumption is that integral coverslip cells must show a definite superiority over conventional glued coverslip cells. The consequences of this assumption provide natural guidelines for selection of candidate coverslip materials, possible fabrication techniques and environmental test end points. Specifically, all coverslip materials that are known to significantly degrade under ultraviolet, proton or electron irradiation must be categorically excluded from consideration. Similarly, all fabrication techniques that are inherently deleterious to the cell structure itself must be rejected. Finally, the environmental and radiation test end points must be at least as severe as those encountered with glued coverslip cells. For ease in comparison, final testing is to be done on cells with 6 mil integral coverslips.



## TABLE OF CONTENTS

<u>Section</u>		<u>Page</u>
	OBJECTIVE . . . . .	iii
1	INTRODUCTION . . . . .	1
2	TECHNICAL DISCUSSION . . . . .	2
	2.1 Stress Analysis . . . . .	3
	2.2 High Vacuum Sputtered Coverslips . . . . .	6
	2.3 Antireflection Coating . . . . .	12
	2.4 Ultraviolet Vacuum Testing . . . . .	16
	2.5 Proton Resistance . . . . .	16
	2.6 Equipment . . . . .	23
3	FUTURE PLANS . . . . .	25

### APPENDIX A

#### OPTICAL ANALYSIS TECHNIQUE



# LIST OF ILLUSTRATIONS

<u>Figure</u>		<u>Page</u>
1	Coverslip Cell Bow (Production Machine) . . . . .	2
2	Best Straight Line Fit of Experimental Cell Bow vs Coverslip Thickness Data . . . . .	4
3	Peak Silicon Stress vs Coverslip Thickness . . . . .	5
4	Optical Transmission Run No. 11 . . . . .	7
5	Optical Transmission Run No. 16 . . . . .	10
6	Optical Transmission Test Run (Production Machine) . . . . .	13
7	Antireflection Coating Effectiveness . . . . .	15
8	Calculated Fraction of Incident Intensity Reflected from Coverslip Cells . . . . .	18
9	Proton Strip Mask . . . . .	21





## LIST OF TABLES

<u>Table</u>		<u>Page</u>
1	Experimental Data Summary . . . . .	17
2	MgF <sub>2</sub> Coating Results . . . . .	19
3	Vacuum UV Storage No. 4 . . . . .	20
4	Strip Irradiation Results . . . . .	22

## SECTION 1

### INTRODUCTION

This report covers two quarterly reporting periods. During the first period, the level of effort on the program was reduced and no separate report was issued for that period.

High vacuum sputtering of integral coverslips has continued in the new enlarged sputtering system shown in the Fourth Quarterly Report. During this period, the system was automated to allow continuous running without an operator. Troubleshooting of the new system resulted in excessive downtime during initial running that is not anticipated to re-occur. The coverslipping results are described in detail in Section 2. The contamination that occurred degraded the cells significantly and did not justify increasing the coverslip thickness beyond 2 mils when the cells were removed for test.

Equipment is being modified for rf and rf-dc reactive sputtering. Satisfactory operation of the rf equipment has not been achieved and as a result an evaluation of commercially-available equipment has been conducted.

While equipment problems have delayed the fabrication of thick integral coverslips, work has continued on testing and evaluation of coverslipped cells. Only  $\text{SiO}_2$  was considered in this work. Two of the major problems are film stress and film quality.

The stress resulting from the high vacuum sputtering technique has been documented. Considerable variation in the stress across the 33 cm sample mounting platen has been observed. Figure 1 indicates the variation in cell bow. This variation is consistently observed and correlates with an asymmetry in the high vacuum sputtering system. It is believed that the correlation may provide an insight into the cause of the stress and a scheme for reducing it.

The quality of the high vacuum sputtered film from the new machine indicated a problem with absorption and an evaluation was conducted. The analysis is discussed in Section 2. One potential source of the problem has been identified and corrections are being made to the system.

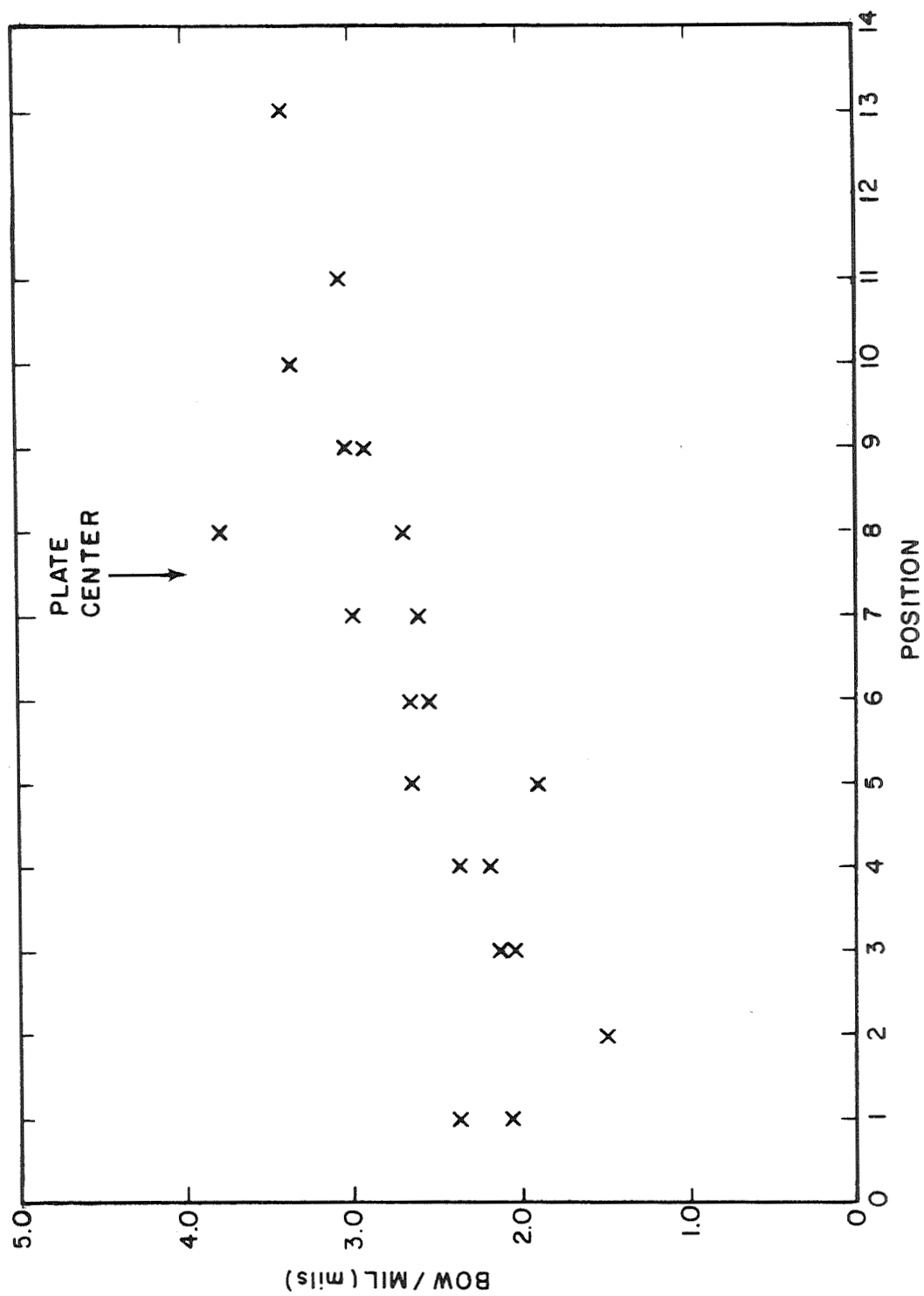


Figure 1. Coverslip Cell Bow - Production Machine

## SECTION 2

### TECHNICAL DISCUSSION

#### 2.1 Stress Analysis

Experimental cell curvature versus coverslip thickness data was presented in Figure 2 of Quarterly Report No. 4. Regression techniques have been used to obtain best fit polynomials for the data. The first and second order best fit polynomials found are:

$$(1) \quad z = 3.45 d - 1.15$$

$$(2) \quad z = 0.15 d^2 + 2.41 d + 0.46$$

where  $z$  is cell bow as measured by the clamped end technique and  $d$  is coverslip thickness. These fitted polynomials have not been forced to pass through the origin. The straight line (1) is a good approximation for the purpose of stress calculation and is shown in Figure 2. This straight line can be taken to represent the IPC high vacuum sputtered integral coverslip results.

The maximum stress,  $S_{\max}$ , in the silicon of a solar cell stressed to radius  $r$  is approximately given by:

$$S_{\max} = \frac{2}{3} \frac{E_s t}{r} \quad (1)$$

where  $E_s$  is Young's modulus of silicon ( $1.24 \times 10^{12}$  dynes/cm<sup>2</sup> for the  $\langle 111 \rangle$  plane) and  $t$  is the silicon thickness. Radius of curvature is related to bow  $z$  as:

$$r = \frac{\ell^2}{2z} \quad (2)$$

where  $\ell$  is the length of the curved edge (2 cm). Introduction of the experimental data best fit straight line into (1) and (2) results in the plot, shown in Figure 3, of maximum silicon stress as a function of slip thickness.

The peak stress in silicon is presented in pounds/square inch for comparison with the stress found by others. While it appears the high vacuum sputtered film is significantly strained, a direct comparison with other data depends on the equation and constants chosen for the calculation.

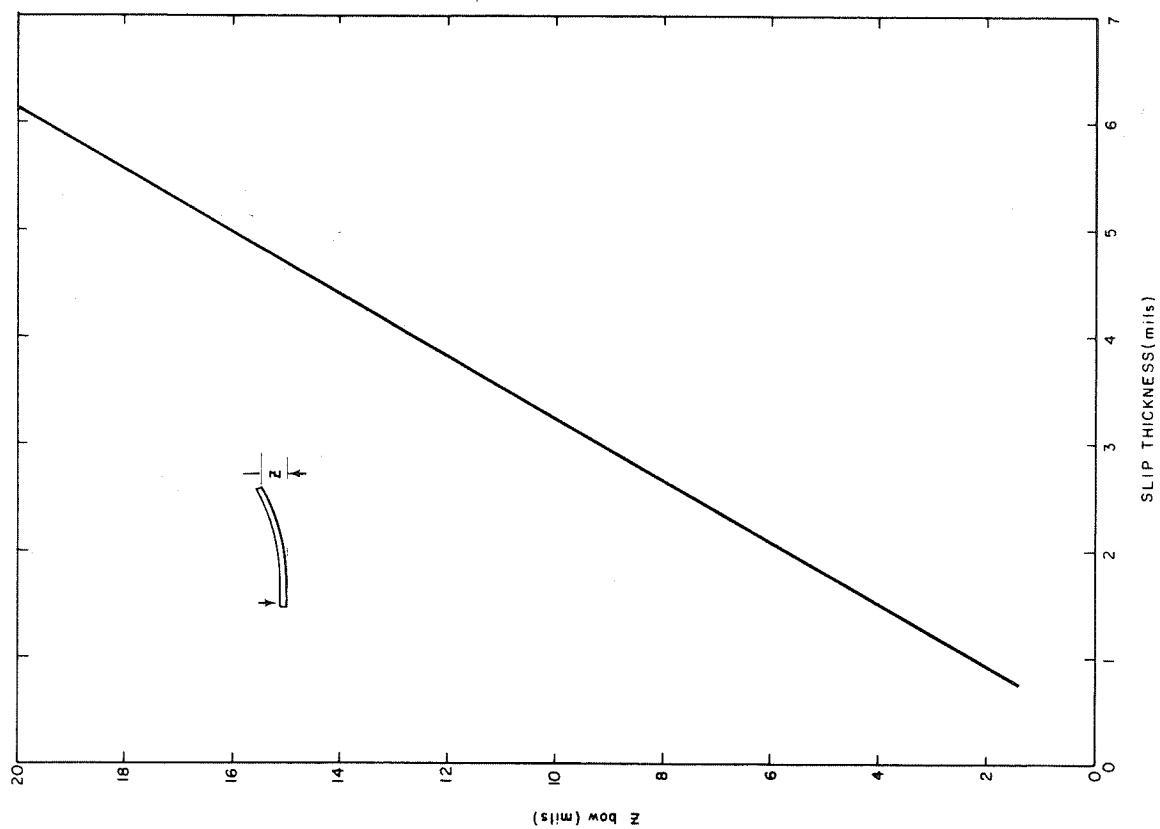


Figure 2. Best Straight Line Fit of Experimental Cell Bow  
vs Coverslip Thickness Data

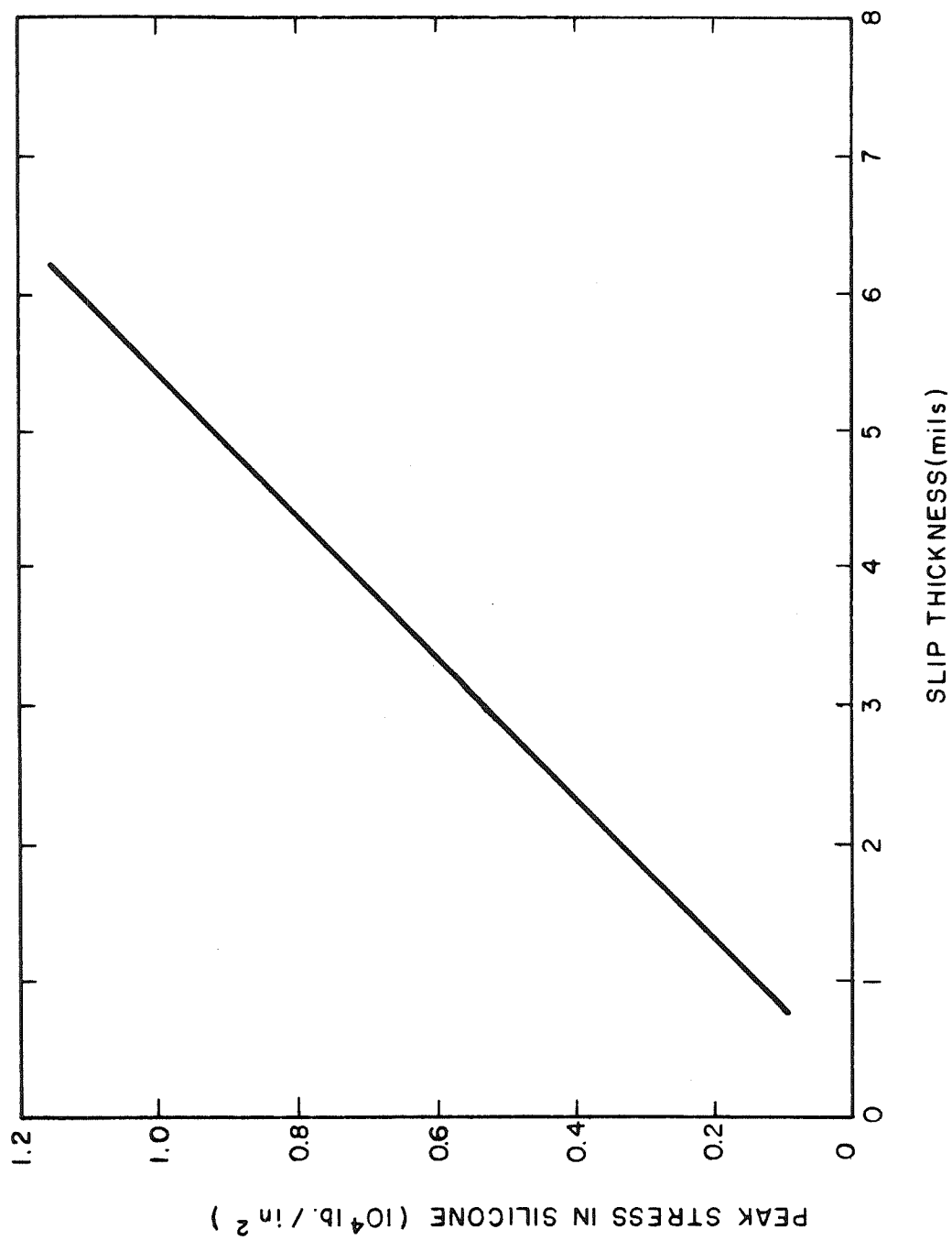


Figure 3. Peak Silicon Stress vs Coverslip Thickness

Coverslipping was begun in the new beam sputtering production coverslipping machine during the quarter. Thick integral coverslips were to be obtained by cycling cells through 2 mil integral coverslipping production runs. When the first 200 hour run was completed, the  $\text{SiO}_2$  indicated a significant yellowing. The cells were removed and electrical tests made. A significant decrease in efficiency was found. In previous coverslipping runs, a slight loss in efficiency has been generally detected when an increase would be expected with the  $\text{CeO}_2$  coating. For the first 200 hour run a significant loss (about 67%) in efficiency was measured.

To determine the quality of the  $\text{SiO}_2$ , an optical analysis has been carried out on these and other samples. The light transmission of  $\text{SiO}_2$  films deposited on Corning No. 7740 fused silica is described for earlier runs, as well as a sample from the production run. The technique is described in Appendix A.

Figures 4a, 4b and 4c display the transmission of a not particularly good early 114 micron thick film (Run No. 11). Figure 4a covers the VIS-UV range (800 to 190  $\text{m}\mu$ ) and illustrates certain features of these films. Most noticeable is a broad absorption peak centered near 560  $\text{m}\mu$ . This broad line dominates film transmission throughout the visible region by producing a rather flat shoulder in the 400 to 600  $\text{m}\mu$  region. While the total absorption of this broad line is rather small, even in this case, its effect on cell response would be quite large. (In Figure 5a, this 560  $\text{m}\mu$  line is barely discernable.) There is a second small, broad absorption line at  $\sim 620 \text{ m}\mu$  that cannot be resolved in Figure 4a. (It is, again, barely discernable in Figure 5a.) In samples like that of Run No. 11, the 560 and 620  $\text{m}\mu$  lines merge to give an absorbing shoulder. Absorption from the 620  $\text{m}\mu$  line has always been observed to be less than or equal to that of the 560  $\text{m}\mu$  line. Some samples suggest there is a third broad absorption line at  $\sim 470 \text{ m}\mu$ . This line is barely apparent in Figure 5a, and is lost in the tailing of Figure 4a.

These three lines are probably due to metal contamination from stainless steel. Their extreme width suggests that the impurity metals are conjugated with varying length chains of Si atoms or  $\text{SiO}_2$  molecules since a simple metal-Si species would be expected to produce sharp absorption lines. Identification of these lines is being pursued.

Figures 5a and 5b are the spectrum scans for an earlier good 21 micron film (Run No. 16). From Figure 5a it is seen that there is some transmission tailing in the 300 to 400  $\text{m}\mu$  region even in a good film. The 300 to 400  $\text{m}\mu$  region of Figure 4a is seen to be heavily absorbing, but without apparent structure. While it is possible that the Run No. 16 film has a specific absorption peak in this region, it is presently thought that this absorption is due either to the broadness of the  $\text{SiO}_x$  absorption in the 200 to 300  $\text{m}\mu$  region or to light

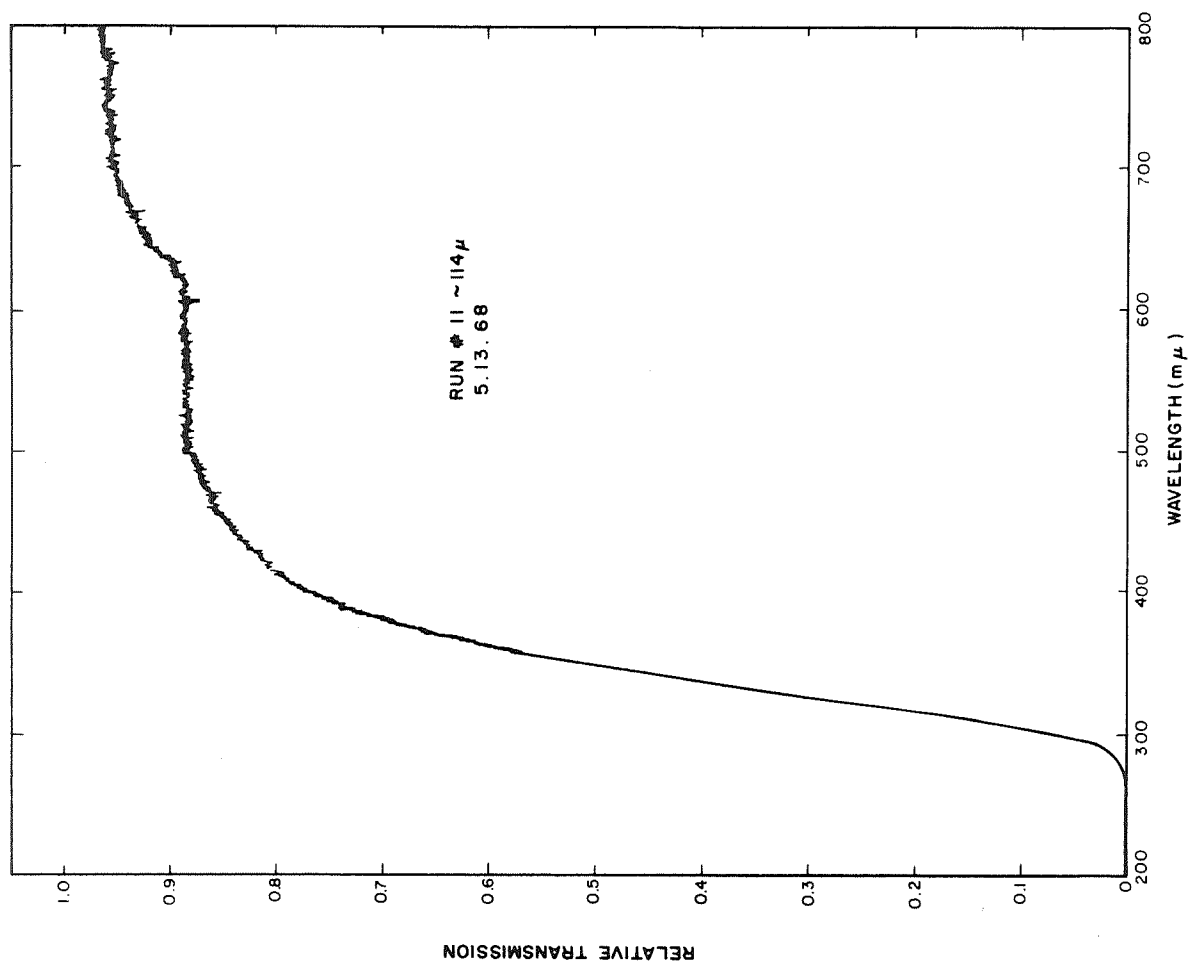


Figure 4a. Optical Transmission Run 11



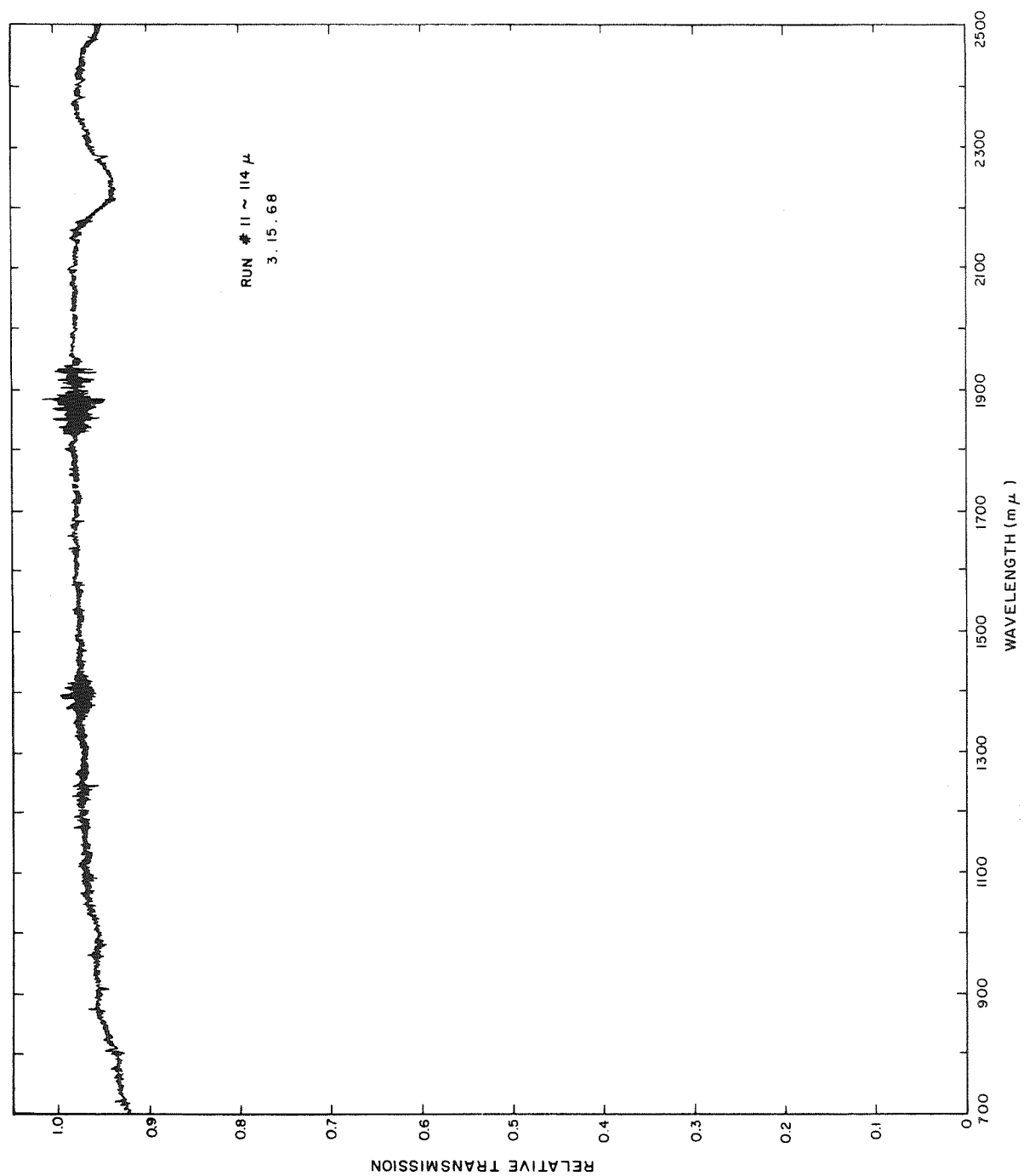


Figure 4b. Optical Transmission Run 11

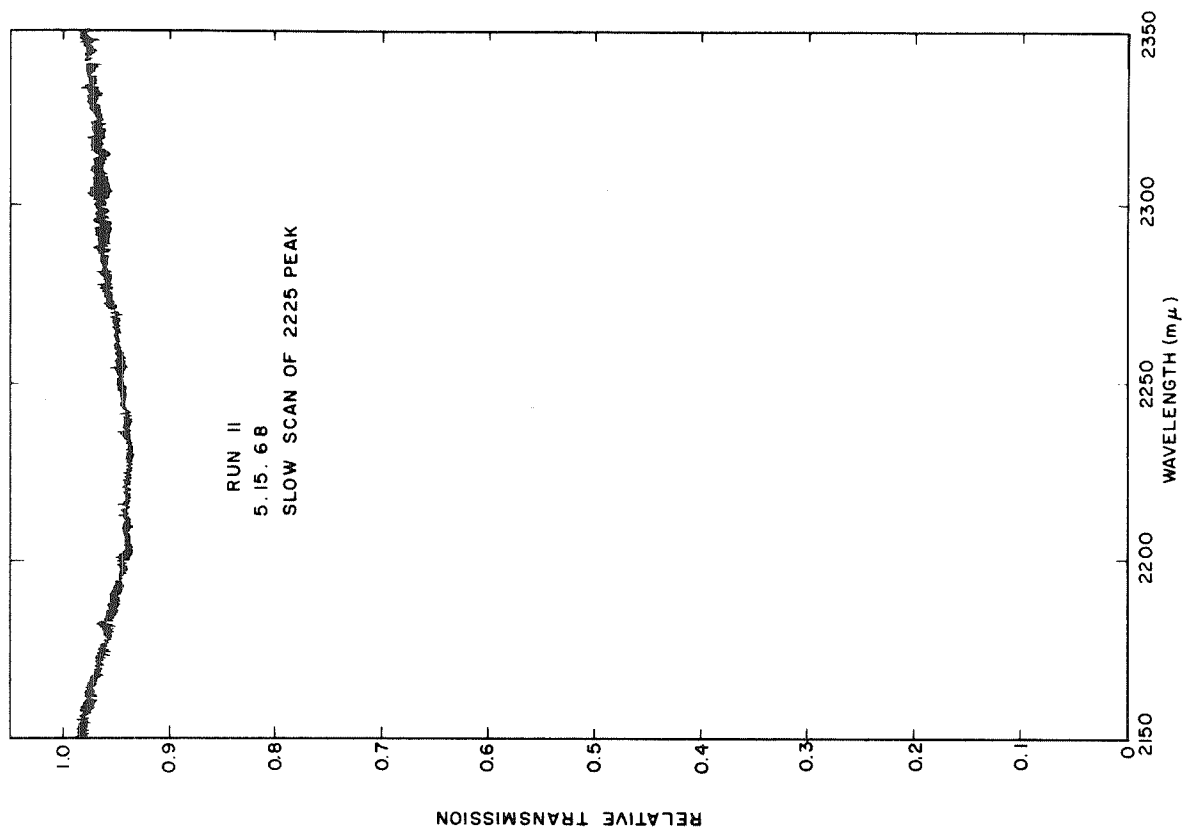


Figure 4c. Optical Transmission Run 11

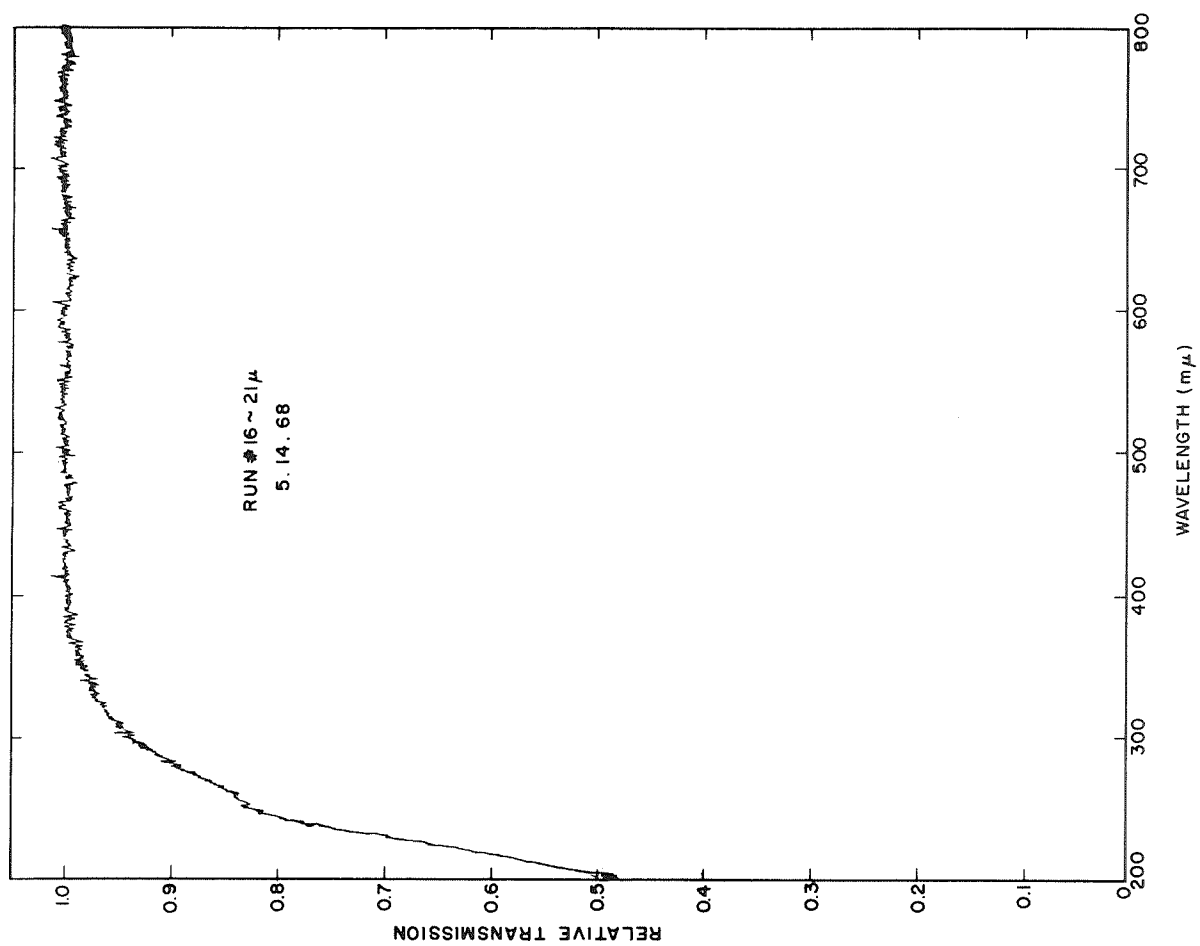


Figure 5a. Optical Transmission Run 16

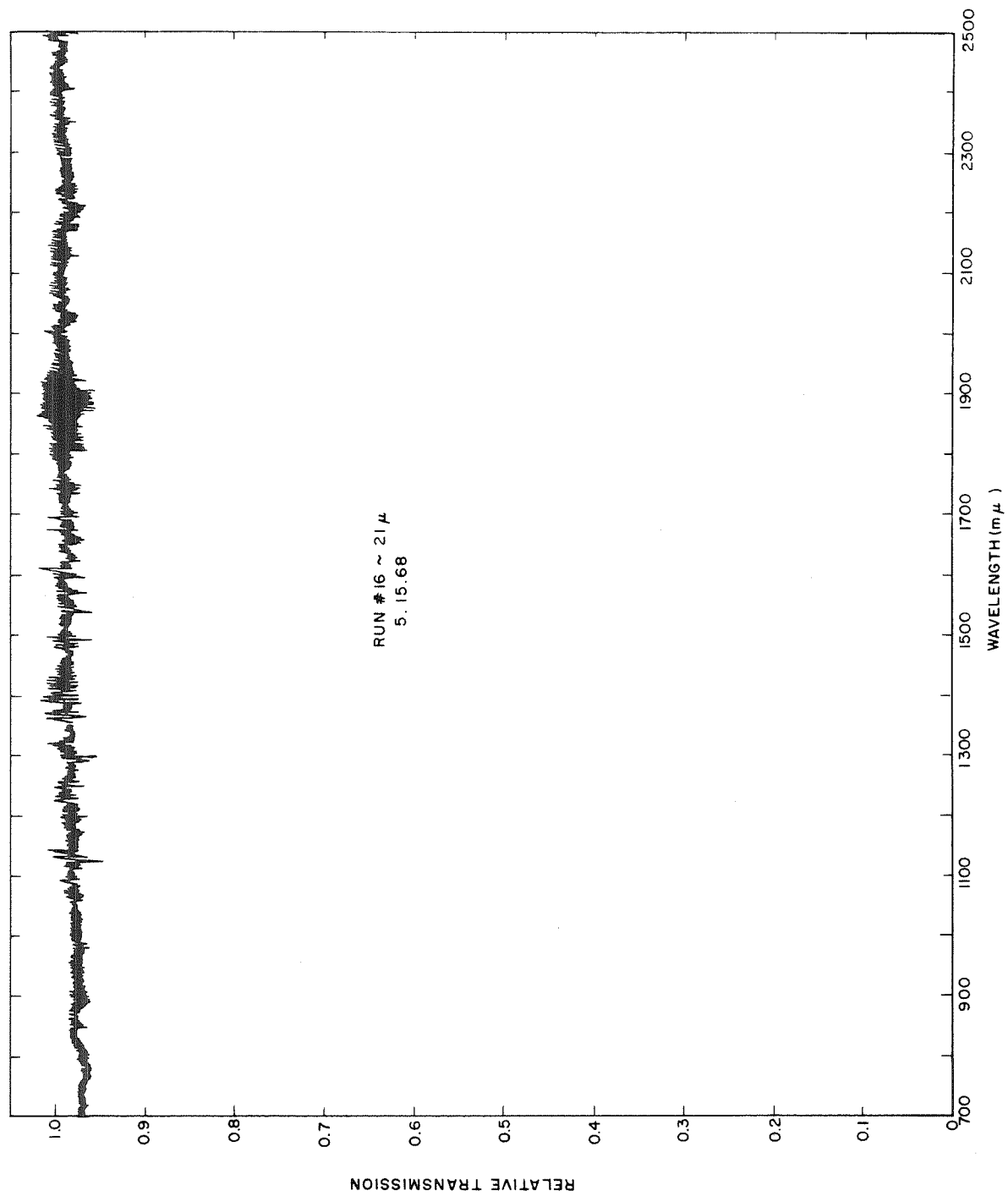


Figure 5b. Optical Transmission Run 16

1-2972

scattering. Reflection measurements that are currently in progress should allow a separation of these two effects. The absorption in the 200 to 300  $\text{m}\mu$  region has been attributed to  $\text{SiO}_x$  in the literature.

Figures 4b and 5b are the near-IR scans of Run No. 11 and Run No. 16, respectively. To  $\sim 1000 \text{ m}\mu$  they are quite similar. Below this point, Figure 4b suggests a slight tailing that is not really seen in Figure 5b. This could, again, be due to light scattering or to an unidentified specific absorption. In both Figures 4b and 5b, the large bands near 1400  $\text{m}\mu$  and 1850  $\text{m}\mu$  are due to atmospheric absorption. (The spectrometer was not purged with dry  $\text{N}_2$ .) The large bands near 2250  $\text{m}\mu$  are characteristic of fused silica. Figure 4c is an expanded trace of the 2250  $\text{m}\mu$  band shown in Figure 4b. Beyond these, there are suggestions of absorption bands at 780 to 790  $\text{m}\mu$ , 990  $\text{m}\mu$  and 1280  $\text{m}\mu$ . They are all small and have not been identified.

Figures 6a and 6b are the scans of a poor  $\sim 58$  micron film from the production coverslipping machine. This film was visibly brownish. (The brown film appearance in polychromatic light is due to heavy absorption of the blue end of the spectrum.) From Figure 6b, it is seen that a relatively heavy absorption extends throughout the entire near-IR region. Superimposed on this are the fine features seen in the Figure 4b and 5b traces. Figure 6a shows this absorption tails rapidly across the VIS-UV region. The essentially flat absorption shown in these last two figures suggests either serious light scattering losses or deposition of a thin metal film, unassociated with the  $\text{SiO}_2$ , at some level in the deposited slip. The cause for this behavior is under investigation.

It is readily seen that this run is quite poor in comparison to Run Nos. 11 and 16, and is, in fact, completely unacceptable. Other production machine test runs, of comparable film thickness, have produced films whose transmission falls between that of Run No. 16 and Run No. 11.

It should be stressed that these spectra have been run for purposes of film analysis and quality control. The apparent transmission observed in the scans is less than would be observed on coverslipped cells, since scattered light is lost from the spectrometer measurements while, due to the small spacing between the scattering centers in the slip and the cell, some of the scattered light would be absorbed in the cell.

### 2.3 Antireflection Coating

Previous discussions in Quarterly Technical Progress Report No. 4 indicate the advantage of the use of  $\text{CeO}_2$  antireflecting coating between the silicon and  $\text{SiO}_2$ . This has been documented by IPC and the pertinent results are shown in Figure 7 which indicates the results of cells taken from two lots one-half of which were antireflective coated with  $\text{CeO}_2$  and one-half coated with

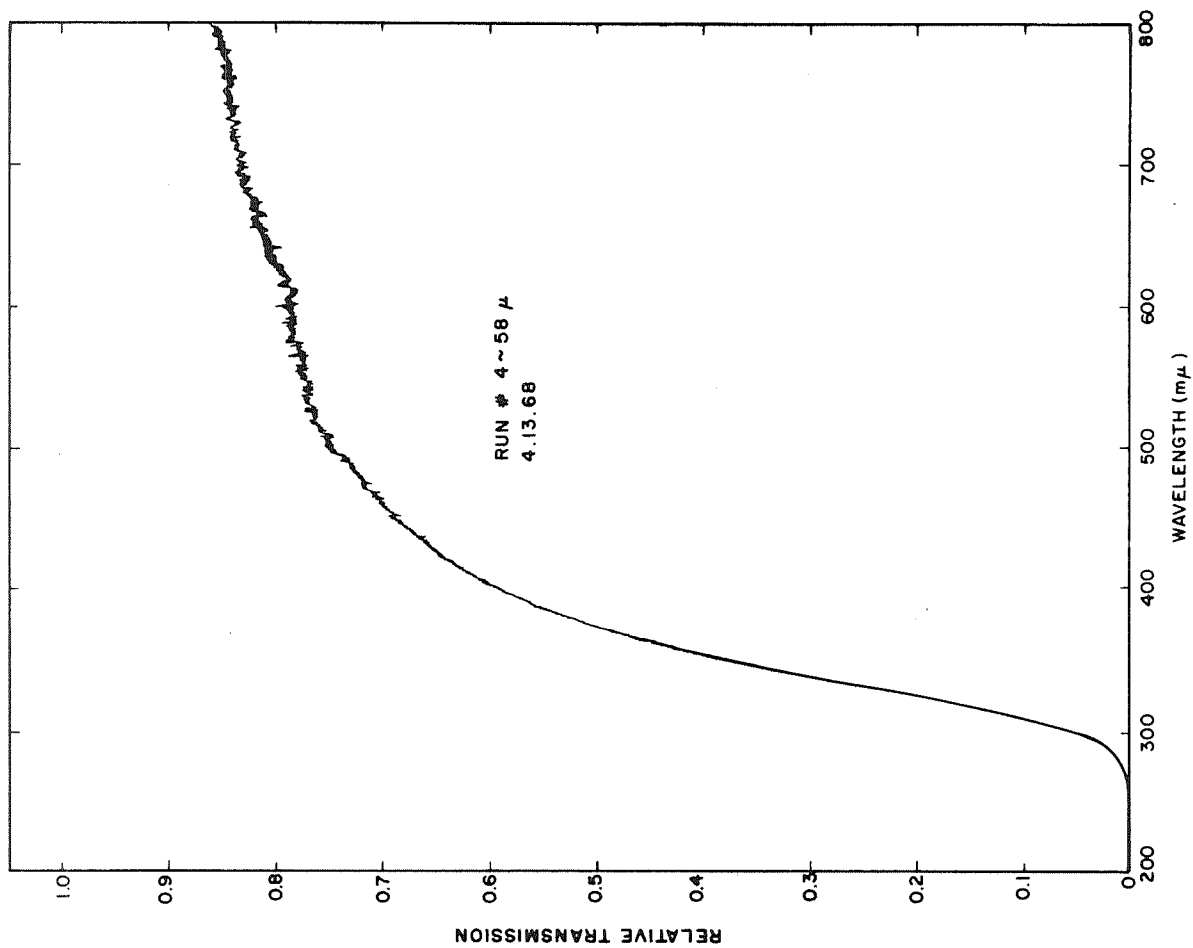


Figure 6a. Optical Transmission Test Run (Production Machine)

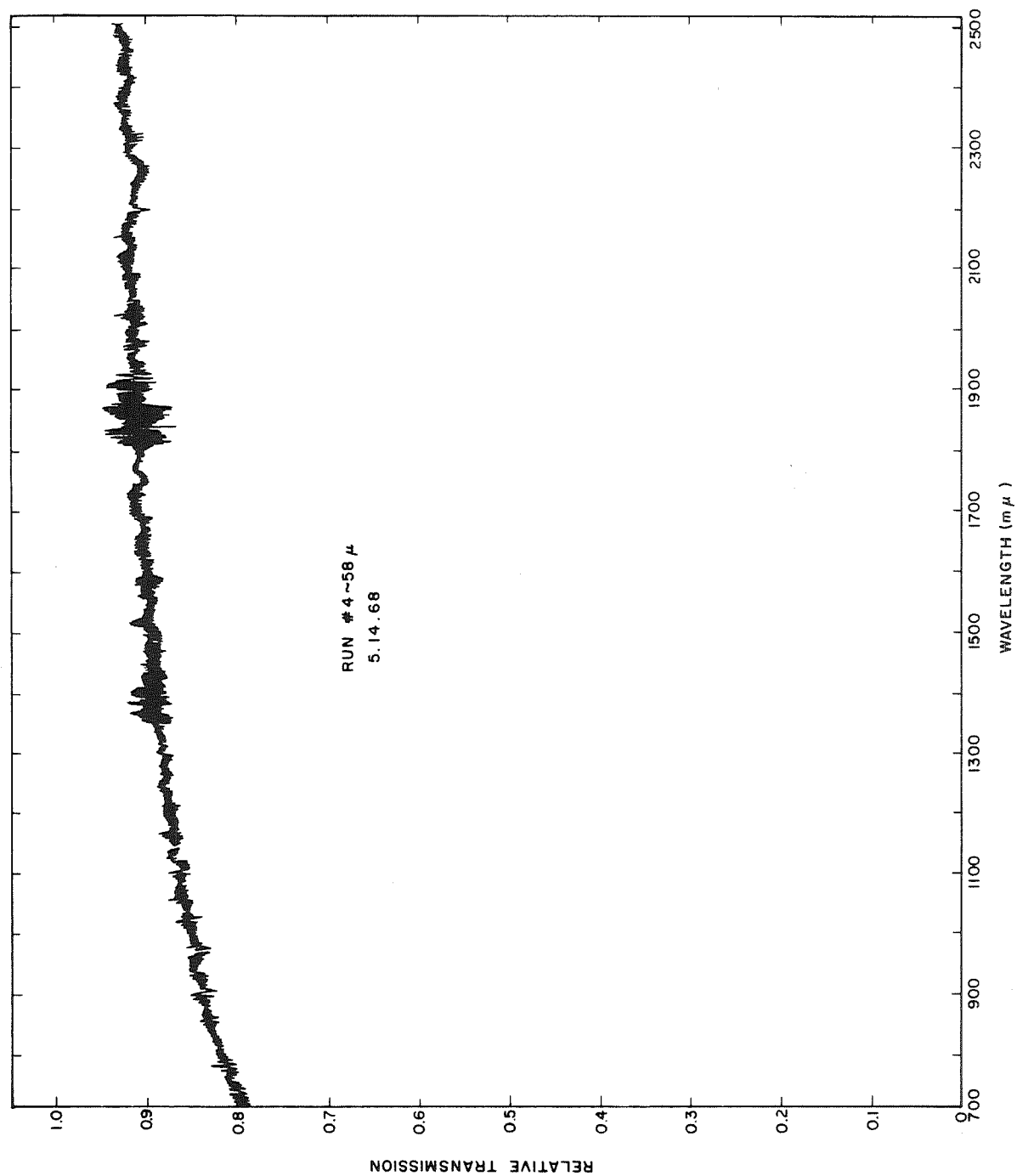


Figure 6b. Optical Transmission Test Run (Production Machine)

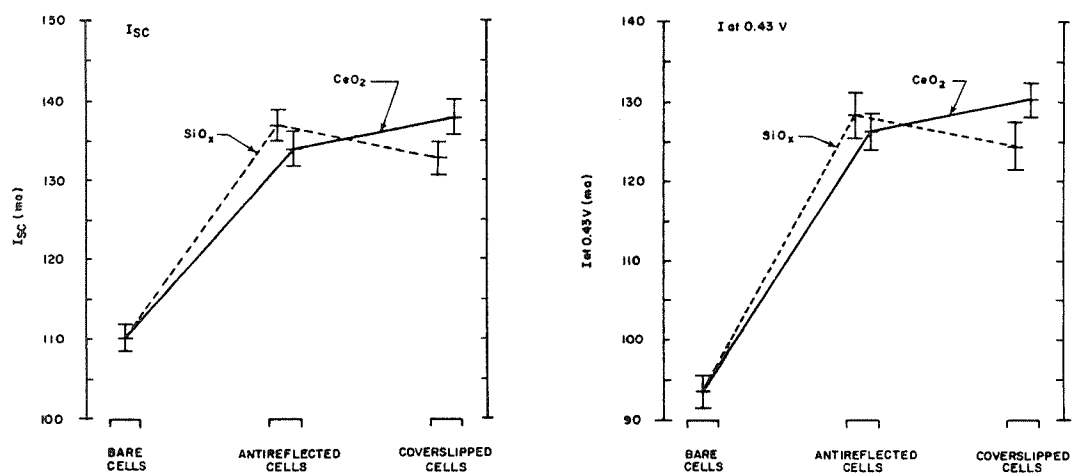


Figure 7. Antireflection Coating Effectiveness



SiO<sub>x</sub>. The data is summarized in Table 1. The results with coverslips were obtained by applying OCLI coverslips of Corning 7940 with GE RTV602.

For integral coverslipped cells, the improvement indicated above has not been consistently demonstrated. In general, the cells have changed little or slightly degraded on application of the coverslip. A large degradation recently observed due to optical absorption has been previously discussed.

The standard glued coverslips have an antireflection coating of MgF<sub>2</sub>. This is a common coating in the optical industry to reduce reflection at quartz air interfaces. An improvement in integral coverslipped solar cells can be obtained by application of MgF<sub>2</sub> to the SiO<sub>2</sub>. The theoretical improvement is indicated in Figure 8. Integral coverslipped cells have been coated with MgF<sub>2</sub> with before and after electrical data listed in Table 2.

#### 2.4 Ultraviolet Vacuum Testing

Another 100°C vacuum-UV test was run during the quarter for 560 hours. The equipment was described in Quarterly Report No. 3. Eight cells were used for the test. Four of the cells had integral coverslips of 2 mil thickness and four had only the CeO<sub>2</sub> antireflection coating. The results of the test are tabulated in Table 3. No measurement degradation was evident.

#### 2.5 Proton Resistance

Quarterly Report No. 4 provided information on the degradation from low energy protons of cells with exposed unsoldered contact bars and indicated the necessity for protecting the back surface contact.

Protection of the contact bar with solder can solve part of the problem. Often with glued coverslips a region of the cell is exposed between the contact bar and cover glass. In application of an integral cover glass it is possible to protect the cell with a coating that partially covers the contact bar reducing the exposed gap to zero.

An example of the degradation that can be expected from an exposed area is indicated in results from Air Force Contract F33615-68-C-1164, where a strip was exposed to 400 kV protons as shown in Figure 9. The results are shown in Table 4 and indicate a degradation in cell efficiency, a slight improvement above 10<sup>13</sup> p/cm<sup>2</sup> in the efficiency has been noted but complete recovery is neither achieved or expected.

Table 1. Experimental Data Summary

			I <sub>sc</sub> (ma)		I @ 0.43 V (ma)	
			Average	Std Deviation	Average	Std Deviation
Bare Cells	CeO <sub>2</sub> Cells	Lot 254 (23 cells)	99.26	1.45	93.78	1.51
		Lot 255 (20 cells)	101.20	1.88	94.50	1.73
		Both Lots (43 cells)	100.16	2.13	94.12	1.64
	SiO <sub>x</sub> Cells	Lot 254 (23 cells)	99.35	1.56	92.87	2.32
		Lot 255 (20 cells)	100.50	1.76	93.65	2.48
		Both Lots (43 cells)	99.88	1.73	93.23	2.40
All Bare Cells (86 cells)		100.02	1.82	93.67	2.09	
Anti-reflected Cells	CeO <sub>2</sub> Cells	Lot 254 (23 cells)	132.91	1.70	125.30	2.05
		Lot 255 (20 cells)	135.15	2.03	127.45	1.85
		Both Lots (43 cells)	133.95	2.16	126.30	2.22
	SiO <sub>x</sub> Cells	Lot 254 (23 cells)	136.65	2.23	127.39	3.06
		Lot 255 (20 cells)	137.25	1.65	129.35	2.13
		Both Lots (43 cells)	136.93	1.98	128.30	2.82
Conventionally Cover-slipped Cells	CeO <sub>2</sub> Cells	Lot 254 (23 cells)	136.52	1.44	129.26	1.68
		Lot 255 (20 cells)	139.60	1.82	131.30	1.98
		Both Lots (43 cells)	137.95	2.24	130.21	2.08
	SiO <sub>x</sub> Cells	Lot 254 (23 cells)	132.61	2.44	123.78	3.38
		Lot 255 (20 cells)	133.15	1.53	125.45	2.37
		Both Lots (43 cells)	132.86	2.07	124.56	3.04

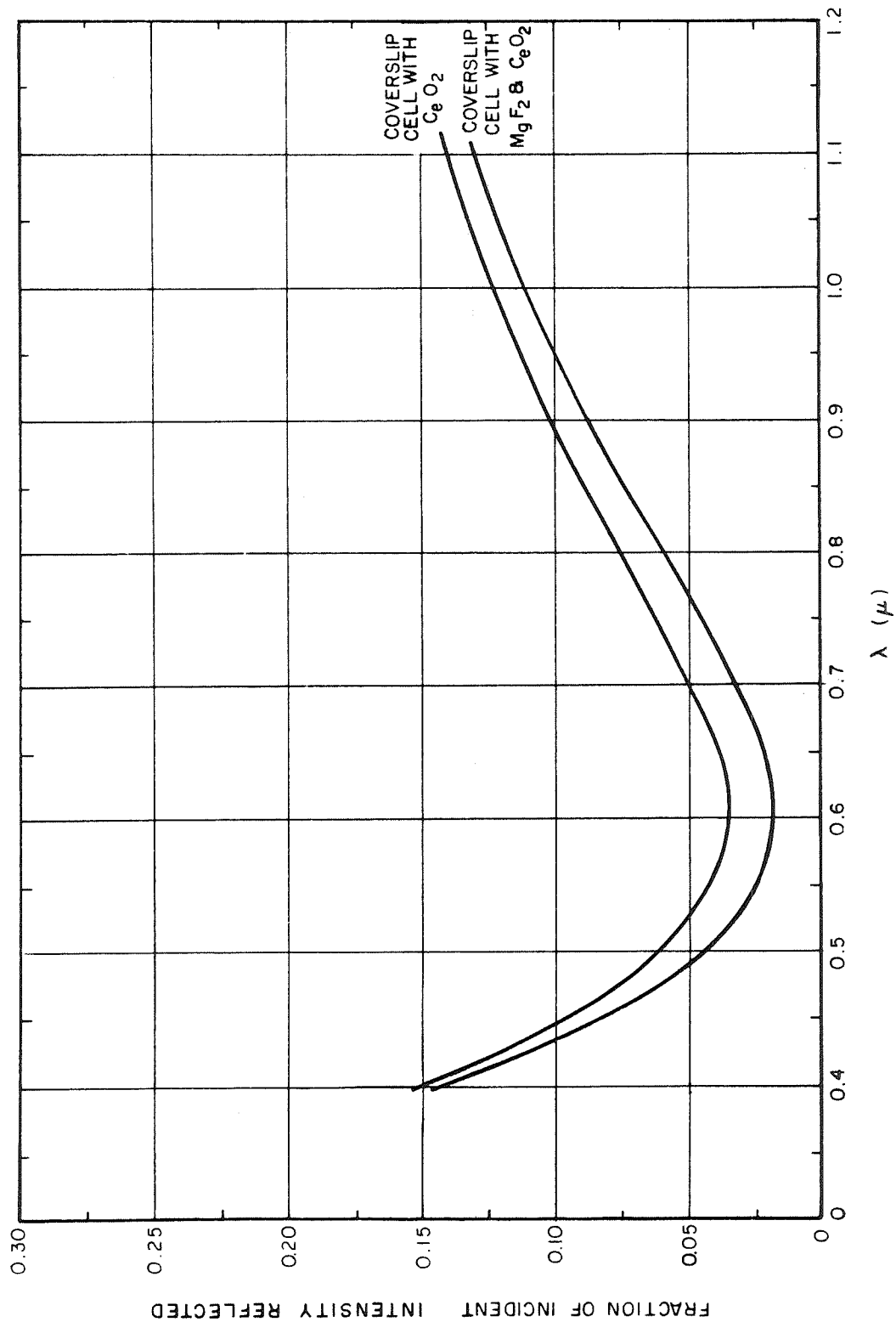


Figure 8. Calculated Fraction of Incident Intensity Reflected from Coverslip Cells

Table 2.  $\text{MgF}_2$  Coating Results

	43, 2 x 2 cm Integral Coverslip Cells Tested		Change after Application of $\text{MgF}_2$
	Arithmetic Mean	Standard Deviation	
$I_{sc}$ Before	135.8 ma	2.2 ma	1.6%
$I_{sc}$ After	138.0	2.1	
$I_{0.43}$ Before	124.3 ma	1.8 ma	1.1%
$I_{0.43}$ After	125.7	1.6	

Table 3. Vacuum UV Storage No. 4

Cell	Type	I <sub>SC</sub>		I <sub>0.43</sub>		V <sub>OC</sub>		$\eta$ at 0.43 Volts	
		Initial (ma)	Final (ma)	Initial (ma)	Final (ma)	Initial (volt)	Final (volt)	Initial (%)	Final (%)
T4-17	Regular no coverslip	138	135	122	122	0.543	0.544	9.9	9.9
T4-18	Regular no coverslip	133	133	120	120	0.544	0.545	9.7	9.7
T4-19	Regular no coverslip	133	131	120	120	0.540	0.538	9.7	9.7
T4-20	Regular no coverslip	135	133	122	123	0.545	0.544	9.9	9.9
T5-2	2 mil coverslip	134	135	126	128	0.548	0.548	10.2	10.2
T5-3	2 mil coverslip	129	132	121	122	0.548	0.549	9.8	9.8
T5-4	2 mil coverslip	135	136	125	127	0.553	0.555	10.1	10.1
T5-6	2 mil coverslip	139	139	127	124	0.549	0.550	10.3	10.3

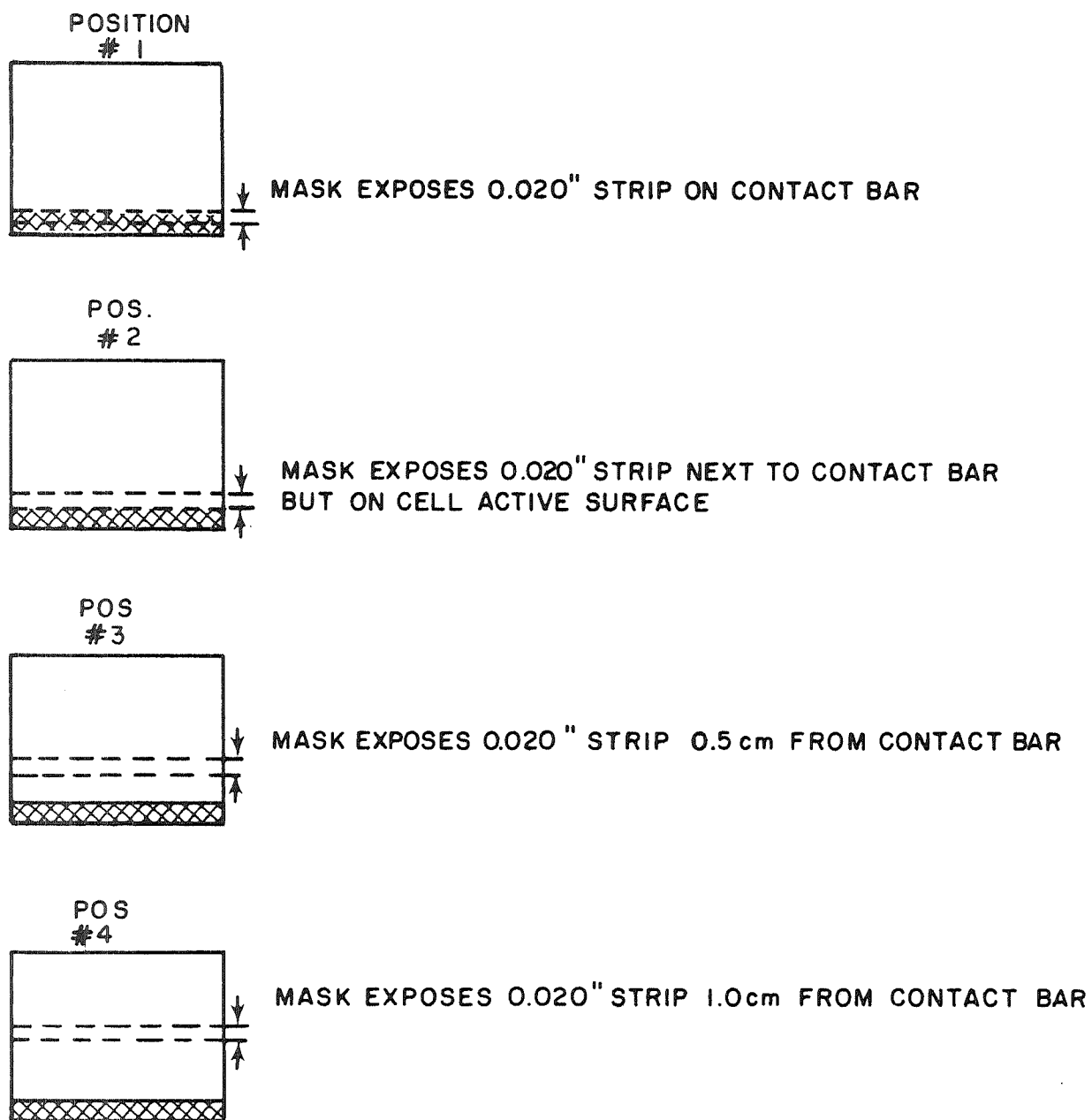


Figure 9. Proton Strip Mask

Table 4. Strip Irradiation Results

Run Number	Mounting Block Temperature	Cell	Position Number	Test	Proton Fluence ( $p/cm^2$ )					
					0 (Initial)	$10^{11}$	$10^{12}$	$10^{13}$	$10^{14}$	$10^{15}$
1	20°C	T4-16	1	$I_{sc}$	133 ma	133 ma	132 ma	131 ma	131 ma	
				$I_{0.43}$	128 ma	127 ma	122 ma	113 ma	112 ma	
				$V_{oc}$	0.554 V	0.551 V	0.545 V	0.544 V	0.541 V	
				$\eta$ at 0.43 V	10.4%	10.3%	9.9%	9.1%	9.1%	
		T4-14	2	$I_{sc}$	134 ma	135 ma	132 ma	133 ma	132 ma	
				$I_{0.43}$	128 ma	127 ma	121 ma	114 ma	118 ma	
				$V_{oc}$	0.548 V	0.544 V	0.538 V	0.536 V	0.542 V	
				$\eta$ at 0.43 V	10.4%	10.3%	9.8%	9.2%	9.6%	
		T4-15	3	$I_{sc}$	133 ma	134 ma	130 ma	130 ma	130 ma	
				$I_{0.43}$	129 ma	129 ma	122 ma	114 ma	117 ma	
				$V_{oc}$	0.562 V	0.555 V	0.550 V	0.548 V	0.552 V	
				$\eta$ at 0.43 V	10.4%	10.4%	9.9%	9.2%	9.5%	
		T4-13	4	$I_{sc}$	136 ma	137 ma	133 ma	134 ma	132 ma	
				$I_{0.43}$	128 ma	129 ma	122 ma	113 ma	117 ma	
				$V_{oc}$	0.551 V	0.549 V	0.546 V	0.543 V	0.550 V	
				$\eta$ at 0.43 V	10.4%	10.4%	9.9%	9.1%	9.5%	
2	20°C	T4-18	1	$I_{sc}$	136 ma		136 ma	135 ma	137 ma	135 ma
				$I_{0.43}$	129 ma		125 ma	114 ma	118 ma	124 ma
				$V_{oc}$	0.553 V		0.543 V	0.536 V	0.540 V	0.545 V
				$\eta$ at 0.43 V	10.4%		10.1%	9.2%	9.6%	10.0%
		T4-20	2	$I_{sc}$	136 ma		135 ma	134 ma	134 ma	132 ma
				$I_{0.43}$	128 ma		119 ma	111 ma	118 ma	119 ma
				$V_{oc}$	0.549 V		0.538 V	0.533 V	0.541 V	0.542 V
				$\eta$ at 0.43 V	10.4%		9.6%	9.0%	9.6%	9.6%
		T4-21	3	$I_{sc}$	138 ma		136 ma	135 ma	135 ma	134 ma
				$I_{0.43}$	130 ma		125 ma	110 ma	118 ma	119 ma
				$V_{oc}$	0.551 V		0.543 V	0.537 V	0.545 V	0.544 V
				$\eta$ at 0.43 V	10.5%		10.1%	8.9%	9.6%	9.6%
		T4-22	4	$I_{sc}$	136 ma		134 ma	133 ma	133 ma	132 ma
				$I_{0.43}$	130 ma		118 ma	108 ma	119 ma	120 ma
				$V_{oc}$	0.553 V		0.547 V	0.542 V	0.550 V	0.549 V
				$\eta$ at 0.43 V	10.5%		9.6%	8.7%	9.6%	9.7%
3	-196°C	T4-26	1	$I_{sc}$	133 ma		133 ma	133 ma	133 ma	
				$I_{0.43}$	128 ma		121 ma	114 ma	115 ma	
				$V_{oc}$	0.554 V		0.546 V	0.539 V	0.543 V	
				$\eta$ at 0.43 V	10.4%		9.8%	9.2%	9.3%	
		T4-27	2	$I_{sc}$	136 ma		134 ma	135 ma	133 ma	
				$I_{0.43}$	129 ma		123 ma	114 ma	118 ma	
				$V_{oc}$	0.550 V		0.543 V	0.538 V	0.544 V	
				$\eta$ at 0.43 V	10.4%		10.0%	9.2%	9.6%	
		T4-28	3	$I_{sc}$	134 ma		132 ma	133 ma	132 ma	
				$I_{0.43}$	129 ma		123 ma	116 ma	119 ma	
				$V_{oc}$	0.552 V		0.545 V	0.541 V	0.548 V	
				$\eta$ at 0.43 V	10.4%		10.0%	9.5%	9.6%	
		T4-25	4	$I_{sc}$	138 ma		136 ma	135 ma	135 ma	
				$I_{0.43}$	130 ma		122 ma	115 ma	120 ma	
				$V_{oc}$	0.553 V		0.547 V	0.544 V	0.549 V	
				$\eta$ at 0.43 V	10.5%		9.9%	9.3%	9.7%	

## 2. 6      Equipment

The dc sputtering system has been modified for rf sputtering. A 7-inch silicon cathode was fabricated by bonding the silicon to a copper cooling plate with a conducting epoxy OHMEX-Ag.

A 1 kW rf induction heating power supply was coupled to the sputtering electrode. Impedance matching was not accomplished and although a glow discharge could be initiated, insufficient voltage could be obtained for significant sputtering.

Modifications in the coupling system as well as a voltage monitoring system are being made on this system. The silicon cathode is temporarily being replaced with a quartz cathode until the system problems are resolved.

In addition to modification to existing equipment, an evaluation of commercially available sputtering equipment is being conducted.





### SECTION 3

#### FUTURE PLANS

Work will continue on deposition techniques for producing thick integral coverslips. Equipment problems should be essentially solved on both the high vacuum sputtering system and rf sputtering system. It is anticipated that a decision will be made next quarter on the company acquisition of a new rf sputtering system to support the reactive sputtering work.

Electron irradiations of the cover glass samples used in the optical analysis are scheduled for the next quarter.



## APPENDIX A

### OPTICAL ANALYSIS TECHNIQUE

Transmission samples were prepared on 1 x 2 cm by 1/32 inch thick silica microscope slides that were mounted in the same manner (silicone grease or tape) as the cells. The  $\text{SiO}_2$  film thickness was inferred from the coverslip thickness of cells surrounding the transmission samples. The transmission data was taken on a Cary Model 14 spectrophotometer operated in the double beam mode with an uncoated piece (1/32 inch thick) of Corning No. 7740 fused silica in the reference beam. The instrument was balanced to 100% T (transmission) with another piece (1/32 inch thick) of fused silica in the sample compartment. For both the VIS-UV and the near-IR portions of the spectrum, the 100% T was set at 800 m $\mu$ .

In order to minimize light scattering effects in the VIS-UV portion of the spectrum, the samples were mounted against the end of the cell holder nearest the phototube. To minimize reflection loss differences between the coated samples and the blank, the samples were mounted with the deposited film facing the phototube. After the data was taken, it was realized that this mounting position maximizes light scattering and reflection loss (if present) effects in the near-IR region since the light path through the instrument is reversed for this region. This error accounts for the 1-3% lower transmission, at 800 m $\mu$ , of the near-IR scans as compared to the VIS-UV scans. The difference is probably all due to light scattering since the refractive index of high vacuum sputtered  $\text{SiO}_2$  has been found to be identical, within experimental error to that of bulk fused silica. (This would cause reflection loss differences to be minimal.)



# DISTRIBUTION LIST

<u>Addressee</u>	<u>Copies</u>
NASA-Goddard Space Flight Center Greenbelt, Maryland 20771 Attention:	
Office of the Director - Code 100	1
Office of the Assistant Director for Administration and Technical Services - Code 200	3
Office of the Assistant Director for Projects - Code 400	1
Office of the Assistant Director for Systems Reliability - Code 300	1
Office of the Assistant Director for Tracking and Data Systems - Code 500	1
Office of the Assistant Director for Space Sciences - Code 600	1
Office of the Assistant Director for Technology - Code 700	1
GSFC Library - Code 252	2
Contracting Officer - Code 247	1
Technical Information Division - Code 250	4
Technical Representative - Code 716	25
NASA Headquarters FOB 10B Washington, D. C. 20546 Attn: Arvin Smith, Code RNW	1
Anderson, Donald NASA/Ames Research Center Moffett Field, California	1
Bachner, Robert L. Solar Systems, Inc. 8241 N. Kimball Avenue Skokie, Illinois 60078	1

<u>Addressee</u>	<u>Copies</u>
Baicker, J. A. Princeton Research and Development Company Box 641 Princeton, New Jersey	1
Barkley, Dwight W. Liberty Mirror, L. O. F. Brackenridge, Pennsylvania 15014	1
Brancato, E. L. N. R. L. Washington, D. C.	1
Chamberlin, R. R. National Cash Register Company Main and K Streets Dayton, Ohio	1
Cherry, William R. NASA/Goddard Space Flight Center Greenbelt, Maryland 20771	1
Cole, Robert L. Texas Instruments Dallas, Texas	1
Cusano, Dominic A. General Electric, R&D Center P. O. Box 1088 Schenectady, New York	1
Dawson, John R. NASA/Langley Research Center Langley Station Mail Stop 188-B Hampton, Virginia 23365	1
Downing, R. G. TRW Systems 1 Space Park Redondo Beach, California	1
Fang, P. H. (Dr.) NASA/Goddard Space Flight Center Greenbelt, Maryland 20771	1

<u>Addressee</u>	<u>Copies</u>
Ferguson, George D. (Jr.) General Electric Carroll Avenue Lynchburg, Virginia	1
Finger, Harold B NASA Headquarters Washington, D. C. 20546	1
Fischell, Robert JHU/Applied Physics Laboratory Silver Spring, Maryland	1
Hamilton, Robert C. Institute for Defense Analyses 400 Army-Navy Drive Arlington, Virginia 22202	1
Hawkins, Kenneth D. Ryan Aeronautical Company Lindberg Field San Diego, California 92112	1
Haynes, Gilbert A. NASA/Langley Research Center Langley Station Hampton, Virginia 23365	1
Holloway, H. Philco Research Laboratory Blue Bell, Pennsylvania	1
Hood, John Dow Corning Corporation Hemlock, Michigan 48626	1
Iles, Peter A. Hoffman Electronics Corporation 4501 Arden Drive El Monte, California	1
Jilg, Eugene T. Communications Satellite Corporation 2100 L Street, N. W. Washington, D. C. 20037	1



<u>Addressee</u>	<u>Copies</u>
Johnson, Carl E. Bellcomm, Inc. 1100 17th Street, N. W. Washington, D. C.	1
Julius, Richard F. Keltec Industries, Inc. 5901 Edsall Road Alexandria, Virginia 22314	1
Kaye, S. Electro-Optical Systems Inc. 300 No. Halstead Street Pasadena, California	1
King, W. J. (Dr. ) Ion Physics Corporation Burlington, Massachusetts 01803	1
Kittl, Emil U. S. Army Electronics Command Attn: AMSEL-KL-PA Fort Monmouth, New Jersey CC -07703	1
Kling, Harry P. Hittman Associates Beltilmore, Maryland	1
Loferski, Joseph J. (Dr. ) Brown University Providence, Rhode Island	1
Marks, Burton S. Lockheed Missile and Space Company Palo Alto, California	1
Massie, Lowell D. AF Aero Propulsion Laboratory APIP-2 Wright-Patterson Air Force Base, Ohio	1
Mlavsky, A. I. (Dr. ) Tyco Laboratories, Inc. Bear Hill Waltham, Massachusetts 02154	1

<u>Addressee</u>	<u>Copies</u>
Mott, James L. Fairchild Hiller Corporation Rockville, Maryland	1
Oman, Henry Boeing Company Seattle, Washington 98166	1
Pearson, Gerald L. Stanford University Stanford, California	1
Potter, Andrew NASA/Lewis Research Center 21000 Brookpark Road Cleveland, Ohio 44135	1
Plauche, Fulton M. NASA/Manned Space Flight Center EP-5 Houston, Texas 77058	1
Ralph, E. L. Heliotek 12500 Gladstone Avenue Sylmar, California	1
Rappaport, Paul RCA Laboratories Princeton, New Jersey	1
Ray, Kenneth A. Hughes Aircraft Company El Segundo, California	1
Reynard, Duncan L. Philco WOL Palo Alto, California	1
Riel, Robert K. Westinghouse Electric Corporation Semiconductor Division Youngwood, Pennsylvania 15697	1

<u>Addressee</u>	<u>Copies</u>
Ritchie, Donald W. Jet Propulsion Laboratory Pasadena, California	1
Schach, Milton NASA/Goddard Space Flight Center Greenbelt, Maryland 20771	1
Schaefer, James C. Harshaw Chemical Company 1945 E. 97th Street Cleveland, Ohio	1
Schlotterbeck, R. S. General Electric Company Lynchburg, Virginia	1
Schwarz, F. C. NASA/ERC 575 Technology Square Cambridge, Massachusetts 02139	1
Shirland, F. A. Clevite Corporation 540 E. 105th Street Cleveland, Ohio 44108	1
Slifer, Luther W. (Jr.) NASA/Goddard Space Flight Center Greenbelt, Maryland	1
Timberlake, Allen B. Battelle Memorial Institute 505 King Avenue Columbus, Ohio 43201	1
Waddel, Ramond C. (Dr.) NASA/Goddard Space Flight Center Greenbelt, Maryland 20771	1
Winkler, Seymour H. RCA/AED P. O. Box 800 Princeton, New Jersey 08540	1

<u>Addressee</u>	<u>Copies</u>
Wise, Joseph F. USAF-APL APIP-2 Wright-Patterson Air Force Base Dayton, Ohio	1
Yannoni, Nicholas F. AF Cambridge Research Laboratories L. G. Hanscom Field Bedford, Massachusetts 01731	1
Wolf, Martin RCA/AED Princeton, New Jersey	1
Marinozzi, D. Optical Coating Laboratories Santa Rosa, California	1
Starkey, Gerald E. (Major) Headquarters USAF AFRSTD Pentagon Washington, D. C.	1
Werth, John J. General Motors Defense Research Laboratories 6767 Hollister Avenue Goleta, California	1